Optimization of Heat-Integrated Crude Oil Distillation Systems. Part III: Optimization Framework

Lluvia M. Ochoa-Estopier and Megan Jobson*

Centre for Process Integration, School of Chemical Engineering and Analytical Science, The University of Manchester, Sackville Street, Manchester M13 9PL, U.K.

* Supporting Information

ABSTRACT: This paper is the third of a three-part series that applies optimization to maximize the productivity and minimize operating costs of heat-integrated crude oil distillation systems. The approach presented in this paper implements simulation models for the distillation process and heat exchanger network (HEN), and HEN retrofit models into the overall optimization framework. The optimization approach is formulated in two levels. In the first level, simulated annealing is used to optimize the operating conditions of the crude oil distillation unit (e.g., distillation products and stripping steam flow rates, pump-around duties and temperature drops, and furnace exit temperatures) and to propose HEN structural modifications (e.g., adding, removing, relocating heat exchangers; adding, removing stream splitters, etc.). The second level is a nonlinear least-squares problem used to enforce HEN constraints. Three case studies illustrate the application of this approach to increase net profit and reduce annualized costs.

1. INTRODUCTION

Refineries today are facing new challenges to meet require-ments with respect to the environment, product quality, and health and safety. Another challenge is to maximize the yield of valuable products in an energy-efficient way so as to maximize profits. Particularly for crude oil distillation, which consumes the energy equivalent of 7−15% of the crude oil processed,[1] heat integration becomes crucial to overcome challenges related to reducing pollutant emissions and improving the energy efficiency of the distillation process. This series presents a new approach to optimize heat-integrated crude oil distillation systems for energy recovery and profit improvement.

Part I[2] of this series presents a new crude oil distillation modeling framework. This framework uses artificial neural networks (ANNs) to calculate stream properties (e.g., temper-atures, enthalpies, heat capacities, true boiling point temper-atures) that describe the separation and energy performance of the distillation unit.

Part II[3] presents a new retrofit approach for heat exchanger networks, particularly those associated with crude oil distillation units (CDUs). The retrofit approach employs simulated annealing (SA) to propose structural modifications to the heat exchanger network (HEN) (e.g., adding, removing or relocating heat exchangers; adding or removing stream splitters), and a nonlinear least-squares problem is solved to handle HEN constraints (e.g., minimum temperature approach, stream enthalpy balance, heat transfer area and utility constraints).

In part III, the distillation and HEN models developed in the preceding parts of this series are implemented in a SA optimization framework to optimize the operating conditions of a distillation unit while proposing retrofit modifications to the associated HEN. The novelty of the work presented in this series comprises three main features: (1) the development of an ANN distillation model for operational optimization purposes, (2) a HEN retrofit model that considers temperature-dependent heat capacities and constraints for the number and type of structural modifications and heat transfer areas, and (3) the simultaneous consideration of the distillation process and HEN into the optimization framework.

A review of previous retrofit and operational optimization approaches for crude oil distillation systems will be presented first. Then, the simulation approach that considers the distillation and HEN models is presented. The optimization framework for the overall distillation system is described next. Three case studies illustrate the application of the optimization framework to increase net profit and to reduce total annualized costs.

2. PREVIOUS WORK ON RETROFIT OF CRUDE OIL DISTILLATION SYSTEMS

Retrofit of heat-integrated crude oil distillation systems has been studied by several researchers. Early retrofit approaches[4,5] rely on the use of the grand composite curve (GCC) to evaluate the energy-performance of distillation systems. Liebmann[4] decomposes the crude oil distillation unit into an indirect sequence of simple columns. Then rigorous simulations facilitate the construction of the GCC, which is used to generate retrofit modifications. Retrofit modifications include changing heat loads of pump-arounds and reboilers, varying stripping steam flow rates, changing column internals, and installing new fractionation units upstream of the main column. The work of Liebmann[4] is conceptually focused and does not include optimization. Sharma et al.[5] compare the GCCs of distillation columns with and without pump-arounds to assess

the effect of increasing heat recovery on the separation performance of the column. In their work, pump-around duties are varied manually to increase heat recovery while maintaining product quality.

Methodologies to perform retrofit and operational opti-mization of distillation systems considering detailed HEN models have been developed.[6−8] In these approaches, the HEN topology (i.e., connections between heat exchanger units and stream splitters in the HEN), inlet and outlet heat exchanger temperatures, heat loads, heat transfer coefficients, and stream heat capacities are taken into account. Zhang and Zhu[6] present a procedure to optimize the operating conditions of the distillation column and to retrofit the associated HEN. In their work, a simple linear distillation model is combined with a HEN retrofit model based on the approach of Zhu and Asante.[9]

Chen[7] develops a framework to perform synthesis, retrofit, and operational optimization of distillation systems. The method applies the column decomposition concept of Liebmann[4] and simplified distillation models based on the Fenske−Underwood−Gilliland (FUG) method developed by Suphanit[10] and extended by Gadalla[11] and Rastogi.[12] The work of Chen[7] extends these simplified models to account for pump-around location on the separation performance of atmospheric units and proposes a new methodology to specify product flow rates and their boiling points in terms of key components and recoveries. Additionally, the HEN design approach of Chen[7] incorporates multisegmented stream data to represent temperature-dependent thermal properties, namely heat capacities.

López C. et al.[8] present a methodology to perform operational optimization of crude oil distillation systems using nonlinear programming (NLP). The distillation model employs second-order polynomial functions, while mass and energy balances are developed for each heat exchanger in the HEN. The approach of López C. et al.[8] optimizes the crude oil blending fractions and operating conditions (e.g., product yields, pump-around flow rates and return temperatures, stripping steam flow rates, etc.) for a system with several distillation units. A detailed HEN simulation model is used to calculate and constrain furnace inlet temperatures and pump-around return temperatures. López C. et al.[8] reports that including a detailed HEN model in the optimization approach produces results that are more practicable and more credible to operations engineers than results from optimizing the distillation units alone.

Optimizing the distillation process and its heat exchanger network is a complex task. There is a trade-off between model accuracy and computational effort. Due to this complexity, approaches that consider retrofit[6,7] typically decompose the design problem into simpler problems. In the first level of the approach of Zhang and Zhu,[6] the main optimization problem calculates the operating conditions (e.g., flow rates and pump-around specifications) of the distillation column. Stream information (e.g., heat capacities, supply and target temperatures) is passed to the second level, where the HEN is retrofitted. The HEN retrofit problem is divided into three problems, namely a diagnostic stage, an evaluation stage, and a cost optimization stage.[9] Deterministic optimization is used in the methodology developed by Zhang and Zhu.[6]

Chen[7] also proposes a two-level approach to retrofit distillation systems. In the first level, simulated annealing is used to perform changes to the distillation system. These changes consider the operational (e.g., flow rates, reflux ratio, heat loads) and structural (e.g., pump-around location, HEN topology) variables of both distillation column and HEN. The distillation system is simulated with the modifications proposed by the SA algorithm. If any HEN constraints are violated, a **repair** algorithm (i.e., the second level) calculates the heat loads that recover HEN feasibility. The repair algorithm proposed by Chen[7] is formulated as a NLP problem and is solved using deterministic optimization.

This work is based on the two-level approach developed by Chen.[7] However, instead of using distillation models based on the FUG method, artificial neural networks are employed. The selection of ANN models to represent the distillation process is discussed in part I[2] of this series of papers, while the HEN retrofit model is discussed in part II[3] of this series.

3. SIMULATION OF THE HEAT-INTEGRATED DISTILLATION SYSTEM

The optimization framework proposed in this paper requires the simulation of the heat-integrated distillation system in order to calculate the objective function and check that constraints are met. This section describes the strategy used to simulate the overall distillation system, incorporating the distillation and HEN models developed in the previous parts of this series.

The heat-integrated distillation system comprises the distillation units and heat exchanger network. The link between the distillation units and HEN is represented by the distillation streams that are heated up or cooled down in the heat exchanger network. Figure 1 represents the many recycle
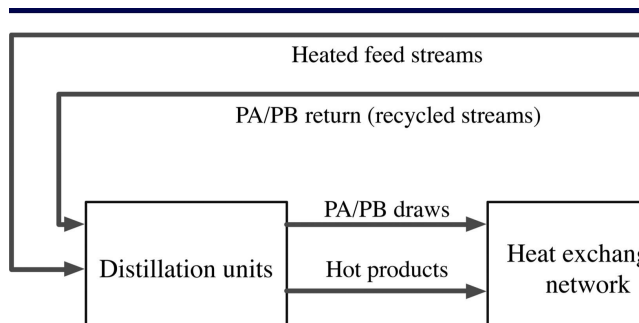
Figure 1. Interactions between the distillation unit and the heat exchanger network.[12] PA, pump-arounds; PB, pump-backs.

streams involved in the heat-integrated distillation system. The presence of these recycle streams complicates the solution of the nonlinear equations that describe the distillation system. If the distillation units and the HEN are simulated together, the calculations for all recycle streams need to converge. This may require the distillation units and HEN to be repeatedly simulated to converge one simulation for the overall system, which is computationally demanding. Furthermore, the iterative procedure used to simulate the overall system may never converge due to the solution of either the distillation units or HEN being infeasible.[12]

Rastogi[12] proposed a sequential strategy to simulate heat-integrated distillation systems. The simulation strategy overcomes convergence problems caused by recycle streams and at the same time is able to capture interactions between the distillation unit and HEN.[7] In the strategy of Rastogi,[12] the distillation units are simulated first for the specified operating conditions. Then, stream data from the simulation of the distillation units are used as specifications to simulate the heat exchanger network. These data consist of supply and target

temperatures, stream enthalpy changes, and heat capacity flow rates for the streams passing through the HEN.

Next, the heat exchanger network is simulated for the given stream data and HEN topology. The HEN simulation model of Rastogi[12] predicts the outlet temperatures of the hot and cold process streams leaving the HEN and utility consumption. Finally, a cost penalty function is assigned to the objective function of the overall design framework to account for the difference between the specified target and calculated outlet temperatures, i.e., violation of constraints.

Chen[7] extended the simulation strategy of Rastogi [12] to check minimum temperature approaches in the HEN as well as stream target temperatures. Before applying penalty functions to penalize infeasible HEN designs (HEN designs that violate stream enthalpy balance constraints and minimum temperature approach constraints), a repair algorithm is used first to calculate the heat loads that recover HEN feasibility. If the HEN design is still infeasible with the new heat loads, a penalty function is then used to help the optimizer seek feasible solutions. Chen[7] shows that more energy-efficient HEN designs are obtained when the feasibility solver is used, compared to using the approach of Rastogi.[12]

The simulation approach of Chen[7] is used in this work with some modifications. In this work, ANN models, rather than simplified models based on the FUG method, are used to simulate the distillation units. The ANN distillation model is regressed against data from rigorous simulations. The resulting ANN model is simpler, more robust, and more computationally efficient than rigorous models, as shown in part I[2] of the series.

The feasibility solver proposed by Chen[7] is extended in this work to consider constraints on heat transfer area and utility consumption (e.g., furnace capacity). Heat transfer area constraints include lower bounds for calculated heat transfer areas, lower and upper bounds for **additional** heat transfer areas, and the total heat transfer area that can be added to the HEN. Additional heat transfer area refers to area that is not yet installed in a heat exchanger but that is needed to meet the specified heat transfer requirements. Knowledge of operating limits of existing heat exchangers can be implemented in the constraints to obtain practicable solutions.

The feasibility solver developed by Chen[7] is also extended to include the optimization of stream split fractions to recover HEN feasibility. The feasibility solver is still formulated as a nonlinear least-squares problem. However, more terms (i.e., heat transfer area and utility constraints) are added to the objective function originally proposed by Chen.[7] Heat loads and stream split fractions are now included as optimization variables of the feasibility solver. For more details on the formulation of the HEN feasibility solver the reader is referred to part II (section 4.2)[3] of this series.

Figures 2 and 3 illustrate the simulation approach proposed in this work. The procedure starts by simulating the crude oil distillation unit. Given a set of specified operating conditions, the feasibility ANN predicts whether these specified inputs are feasible. Here, the feasibility of the distillation unit refers to inputs that result in converged rigorous simulations.[2] If the distillation inputs are feasible, the ANN distillation model predicts stream data used to evaluate constraints on product quality and hydraulic conditions and to simulate the heat exchanger network. If the distillation inputs are infeasible, the overall simulation procedure stops as there are no available results to simulate the HEN (see Figure 2). Figure 3a illustrates the simulation procedure for the distillation unit. The
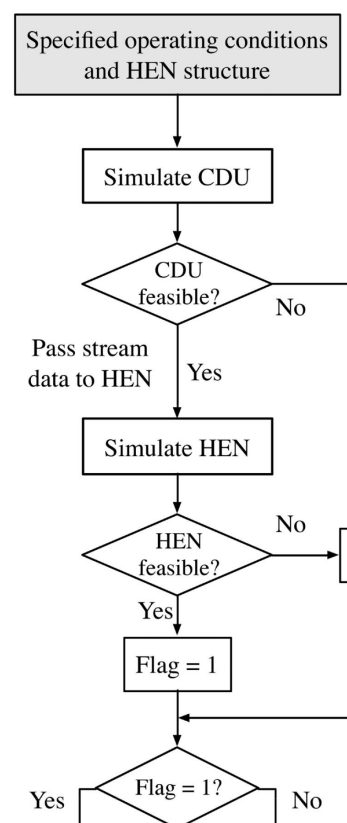
Figure 2. Flowchart for the simulation of the heat-integrated distillation system.

distillation simulation model provides the stream data needed to simulate the HEN, including supply and target temperatures, and enthalpy changes of all process streams involved in heat integration. Stream data for HEN simulation also include the parameters used to model temperature-dependent thermal properties. Temperature-dependent thermal properties, particularly heat capacity flow rates (CP), are considered in the HEN model to obtain meaningful estimations of energy requirements and stream temperatures.[2]

Once results from the distillation process simulation are available, the heat exchanger network is simulated. Figure 3b illustrates this procedure. Given a set of specified operating conditions and HEN topology, the mass and energy balance equations (i.e., the HEN simulation model) are solved. The HEN simulation model calculates the mass flow rates and temperatures in the network. These results are used to evaluate the feasibility of the HEN. Here, HEN feasibility refers to designs that meet constraints related to the minimum temperature approach, stream enthalpy balances, heat transfer areas, and utility consumption. If any of these constraints is violated, the HEN feasibility solver computes new heat loads and split fractions that regain feasibility. The HEN design, and thus the distillation system design, are rejected if the solver is unable to achieve network feasibility. Figure 2 shows the implementation of the distillation and HEN models into the overall simulation procedure.

4. OPTIMIZATION-BASED DESIGN APPROACH

Two different scenarios have been explored in this series so far. In the first scenario,[2] the operating conditions of a distillation unit are optimized without including a detailed HEN model. In
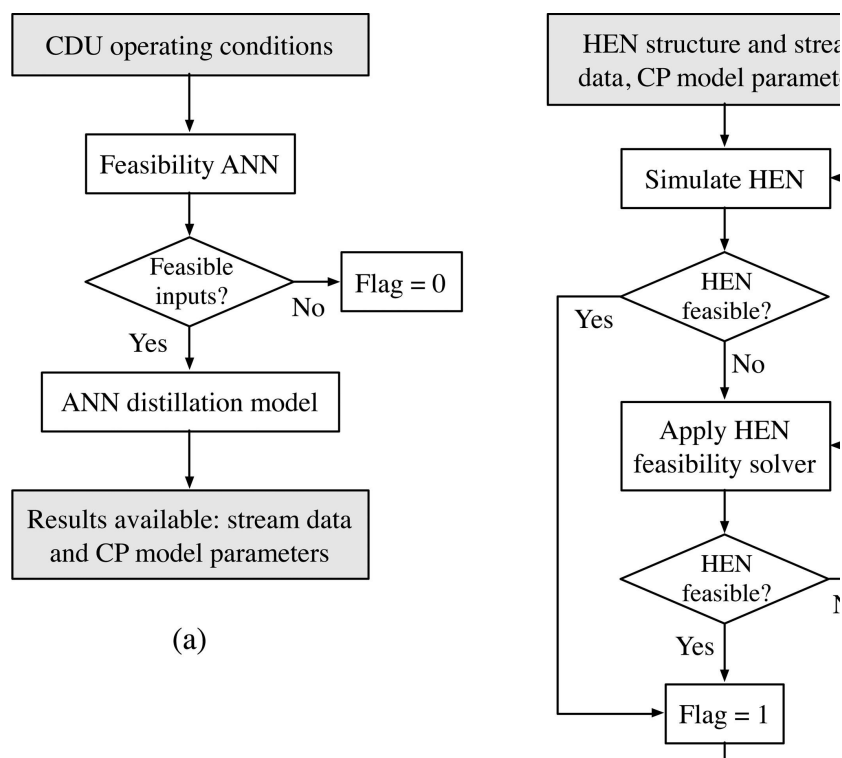
Figure 3. (a) Flowchart for the simulation of the distillation process. (b) Flowchart for the simulation of the heat exchanger network.

this scenario, pinch analysis (using the GCC) is used to calculate utility consumption. In the second scenario,[3] HEN retrofit is performed without considering changes to the distillation process. Neither of these scenarios take into account the synergy between the distillation process and heat recovery network, thus cost-effective design solutions may be missed. Furthermore, optimizing the distillation process without considering the HEN details may produce impractical solutions; that is, operating conditions may not be accom-modated in the distillation system.[8]

This paper explores a third scenario, in which the distillation process and HEN are considered together in the optimization framework. The proposed framework optimizes the operating conditions of the distillation unit and proposes a retrofitted HEN that is able to accommodate the changes made to the distillation process. The optimization framework used in this work is based on the one developed by Chen.[7] Simulated annealing is used as the main optimization algorithm. The simulated annealing algorithm used in this work is described in the second part of this series[3] and has been coded in MATLAB.[13] The advantages and limitations of this optimiza-tion algorithm are also discussed in the second part of the series.

4.1. Objective Function. The role of optimization-based design approaches is to systematically select the best design option from a set of available alternatives. Typically, selection is done based on economic indicators such as product revenue, operating costs, and capital investment. Other criteria can also be used, such as CO_2 emissions reduction,[11] separation efficiency,[14] etc. The criteria used to identify an optimal design depend on the design objective. For example, if the purpose is to perform retrofit to reduce utility consumption, then operating costs and capital investment to retrofit the process should be considered. If the purpose is only to optimize the

operating conditions of an existing process, then no capital investment is necessary, as no changes to the process configuration will be carried out.

In this work, the cost-effectiveness of the heat-integrated distillation system is the criterion used to identify the best design option. The indicator used to assess the cost-effectiveness of the distillation system is the net profit (NP), which is defined as product revenue less the total annualized cost (TAC):

$$NP = \sum_{i=1}^{N_{prod}} C_{prod,i} F_{prod,i} - TAC \tag{1}$$

where C_{prod} and F_{prod} refer to the prices and flow rates of each distillation product i, respectively. N_{prod} is the total number of distillation products. The total annualized cost is defined as the sum of the operating cost (OC) and annualized capital cost (ACC). The operating cost of a crude oil distillation system includes the cost of the crude oil feed, the cost of stripping steam, and the cost of hot and cold utilities. These utilities commonly include fired heating, steam, cooling water, and air. The operating cost can thus be defined as

$$OC = C_{crude} F_{crude} + \sum_{i=1}^{N_{stm}} C_{stm,i} F_{stm,i} + \sum_{j=1}^{N_{util}} C_{util,j} F_{util,j} \tag{2}$$

where C and F refer to prices and flow rates, respectively. Subscripts crude, stm, and util refer to the crude oil, stripping steam, and utilities, respectively. N_{stm} is the total number of stripping steam streams, and N_{util} is the total number of utility streams. Note that different flow and cost units (e.g., kmol/h, bbl/d, etc. for material flow rates; MW, W, etc. for heat flow rates) can be used as long as all the terms in eq 1 and eq 2 have consistent units. For HEN retrofit, capital costs include the cost

Table 1. Unit Prices of Crude Oil and Distillation Products

item	end product	end product prices[a] ($/bbl)	downstream processes	downstream operating costs ($/bbl)[15]	intermediate product prices ($/bbl)
light naphtha	gasoline	103.5			103.5
heavy naphtha	gasoline	103.5	hydrotreating, catalytic reforming	10.8	92.7
light distillate	jet fuel	99.2	hydrotreating	0.2	99.0
heavy distillate	diesel	96.8	hydrotreating	0.2	96.6
residue	residue fuel oil	61.3			61.3
crude oil		79.6[b]			79.6

[a]Based on the price of crude oil.[15] [b]Spot price of Brent crude oil in 2010, taken from EIA.[19]

of modifying existing equipment (e.g., heat transfer area enhancement, repiping heat exchangers, etc.) and the purchase of a few items of new equipment.

The calculation of each cost component in eqs 1 and 2 is described as follows:

• Prices of crude oil and distillation products: The prices of crude oil and crude oil products are unique for each refinery. These prices depend on many factors such as the type of crude being processed, the quality of the products, the geographic location of the refinery, etc. Uncertainty and time-dependence of prices, while very important for refinery planning and operations, have not been addressed in this work. Thus, it is difficult to estimate the prices of crude oil and crude oil products (final and intermediate) for benchmark problems such as the ones presented in this work. Maples[15] presents a procedure to predict the transfer prices of intermediate products and final prices of crude oil products based on the price of crude oil and estimates of typical processing costs of each unit operation in the refinery.

The procedure of Maples[15] is used in this work to estimate the transfer prices of the distillation products. First, the prices of the end products of the refinery are estimated by multiplying the price of crude oil by price factors. Then, the cost of processing the distillation products to produce the final refinery products is calculated. For those distillation products that do not need downstream processing, the price of the end product is the price of the corresponding distillation product. However, if the distillation product is processed in downstream operations, the cost of downstream processing is subtracted from the end product price. Table 1 lists the unit prices of the crude oil and distillation products used in this work. The cost of the crude oil and distillation products are calculated using the unit prices and the calculated flow rates.

• Stripping steam costs and hot and cold utility costs: The prices for stripping steam and hot and cold utilities are taken from Chen.[7] The cost of stripping steam is obtained using the unit price and the flow rate. The cost of hot and cold utilities is calculated from the unit cost (given in cost per unit of energy) and the demand for each utility.

• Capital investment due to HEN retrof it modif ications. The cost of structural modifications for the existing HEN is taken from Gadalla.[11] The cost of new heat exchangers and additional area for existing heat exchangers is calculated using the following relation:

$$\text{Cost} = A + B \times \text{Area}^C \quad (3)$$

The values of the parameters A, B, and C used by Gadalla[11] were regressed against data collected from Douglas,[16] Peters, and Timmerhaus[17] and SPRINT (V1.6).[18] For existing heat exchangers, these values are A($) = 0, B($/m^2) = 1530, and C

= 0.63, where the heat transfer area is in m^2. For new heat exchangers, A($) = 13000. Note that different sets of parameters can also be used. The cost of repiping and resequencing is defined as fixed cost per modification. No costs have been assigned to the modification of stream splitters. More detailed cost models can also be included to consider problem-specific details of pipe diameters, pipe lengths, pump capacity, etc., at the expense of computational complexity. The total capital investment required to retrofit the HEN is annualized using the specified interest rate and project life.

4.2. Constraints. The constraints implemented in the optimization framework consider both the distillation process and the heat exchanger network. These constraints are described in detail in the previous parts of this series.[2,3]

The constraints considered for the distillation process include the lower and upper bounds of the optimization variables (the operating conditions of the distillation unit), T5% and T95% TBP (true boiling point) temperatures, and flooding percentage in the column (see part I[2] for more details). The constraints considered for the HEN relate to the number and type of structural modifications that can be performed to the HEN, heat transfer area, utility consumption, minimum temperature approach, and stream enthalpy balances. The structural HEN modifications considered in this work include adding a new heat exchanger, removing an existing heat exchanger, repiping and resequencing a heat exchanger, adding a new stream splitter, and removing an existing stream splitter. The implementation of these CDU and HEN constraints into the optimization framework is described as follows:

• The constraints on the CDU operating conditions are implemented as parameters of the SA algorithm. The SA algorithm varies the operating conditions of the CDU. For each of these optimization variables, new values are randomly chosen between their lower and upper bounds.

• The constraints on the T5% and T95% TBP temperatures and flooding percentage in the column are implemented as penalty functions in the objective function (eq 1). The penalties are calculated as follows:

$$\text{Penalty}_i = \gamma_i (y_i - y_i^{lb})^2 \quad \text{if } y_i < y_i^{lb} \quad i = 1, 2, ..., N_{\text{prod}} \quad (4)$$

$$\text{Penalty}_i = \gamma_i (y_i - y_i^{ub})^2 \quad \text{if } y_i > y_i^{ub}$$

$$i = 1, 2, ..., N_{\text{prod}} + N_{\text{sections}} \quad (5)$$

where y refers to the T5% and T95% TBP temperatures of the N_{prod} distillation products and the flooding percentage for the N_{sections} sections in the CDU. Superscripts lb and ub indicate the lower and upper bounds, respectively, and γ_i are penalty factors that ensure that all terms are scaled and given the same
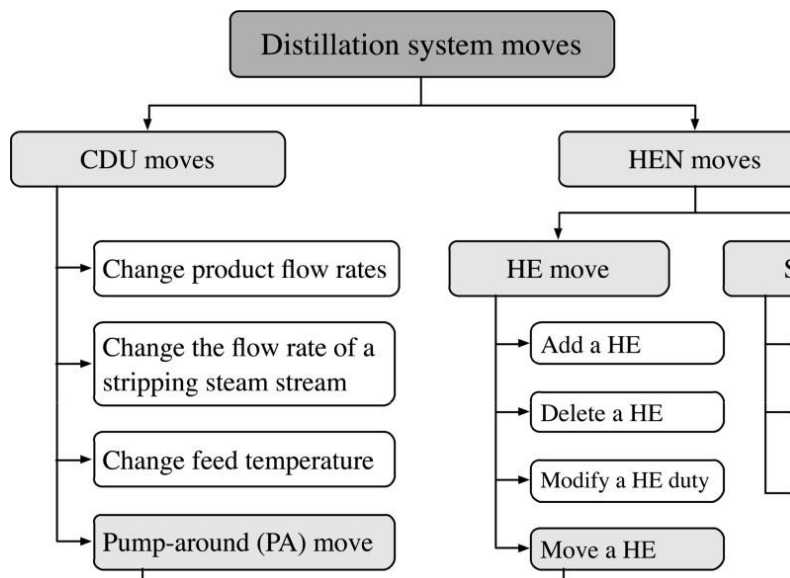
Figure 4. Degrees of freedom for design. HE, heat exchanger; SP, splitter.

importance during optimization. As indicated in eq 4, no lower bound is imposed on the flooding percentage in this work. Note that other properties relevant to the refining industry can be used to control product quality such as Reid vapor pressure, density, viscosity, etc. These properties can be easily considered in the ANN distillation model, as the data are readily available when performing rigorous simulations during the sampling stage of the ANN modeling framework.[2]

• Constraints on the total number of modifications made to the HEN structure are implemented as parameters of the SA algorithm. A set of counters is used to keep track and constrain the total number and type (e.g., adding heat exchangers, removing and relocating heat exchangers, etc.) of structural modifications made to the HEN. A counter is assigned to each type of structural modification, and the maximum value for this counter is specified. The counters are updated each time the SA algorithm accepts a structural modification made to the HEN. If a counter reaches its maximum allowed value, the correspond-ing type of modification becomes unavailable to the SA algorithm; that is, the type of modification is removed from the set of possible modifications that can be selected by the SA optimizer. This type of modification becomes available again if a structural modification of the same type is reverted; e.g., a new heat exchanger is removed from the HEN, a previously repiped heat exchanger is repiped again to its original location, etc.

• The designer can specify the number and type of HEN structural modifications that can be performed to each process stream in the HEN. This includes the specification of forbidden stream matches and the maximum number of heat exchangers and splitters per stream. These constraints are used by the HEN retrofit model (described in part II, section 4.1[3]) to select the stream candidates for the following topology modifications: add heat exchanger, repipe a heat exchanger, and add a stream splitter.

• The type of structural modifications that can be performed on each heat exchanger and splitter can also be constrained. The designer can specify the heat exchangers, and splitters that cannot be removed. It is also possible to specify the heat exchanger side (i.e., hot side or cold side) that cannot be repiped or resequenced. These constraints are used by the HEN retrofit model to select the heat exchanger and stream splitter candidates for the following topology modifications: remove, repipe and resequence a heat exchanger, and remove a stream splitter.

• Constraints on heat transfer area are implemented in the objective function of the HEN feasibility solver described in part II (section 4.2).[3] These constraints consider the total additional area that can be installed in the HEN, the additional area that can be installed for each heat exchanger, and the calculated heat transfer area of each heat exchanger.

• Constraints on utility consumption. These constraints are used to represent the availability of utilities, for example, furnace capacity. These constraints are also implemented in the HEN feasibility solver.

• Minimum temperature approach and stream energy balance constraints. Minimum temperature approach (T_{min}) constraints guarantee the minimum driving force for heat transfer. Stream energy balance constraints ensure that the stream target temperatures in the HEN are met. These constraints are implemented in the HEN feasibility solver.

4.3. Optimization Variables. The optimization degrees of freedom of the heat-integrated distillation system are included in the simulated annealing moves. The moves represent the various types of alterations that can be carried out by the SA algorithm. In this case, the SA moves include modifications to the operating conditions of the CDU and structural modifications to the HEN. These optimization degrees of freedom are represented in the form of a move tree, which is illustrated in Figure 4. A probability is assigned to each move in the move tree (boxes with no shading). For each iteration of the SA algorithm, a move is selected based on the assigned probabilities and the generated random number. The sum of all move probabilities must be one.

The move probabilities bias the search process of the SA algorithm, giving more importance to those variables that have more influence on the performance of the system. Practical issues, such as the difficulty of implementing a certain type of modification, safety, etc., can also be considered to select the values of the move probabilities. The selection of the move
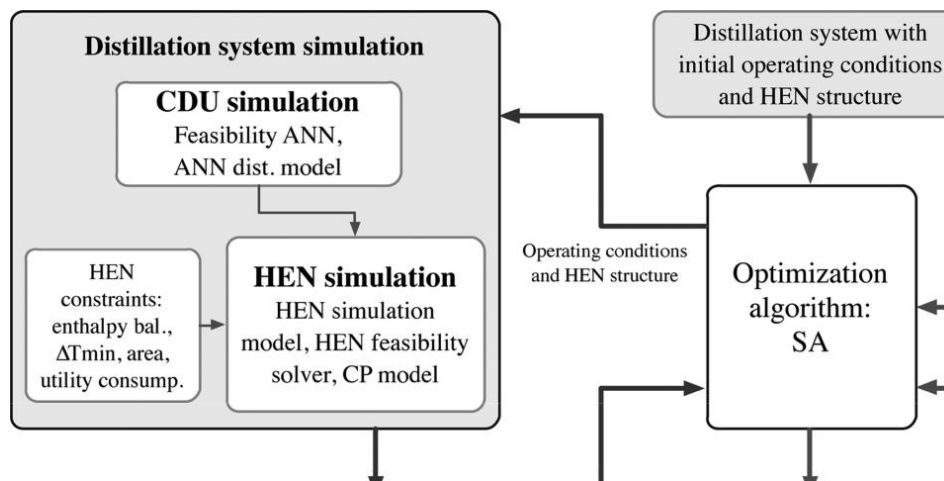
Figure 5. Optimization framework.

probabilities is case-dependent, and several tests may be carried out to select the values that lead to a computationally efficient optimization.

The SA moves related to the distillation process are described below. The SA moves related to the heat exchanger network are described in part II (section 4.1.3).[3]

1. **Change the product flow rates**. In this move, the flow rates of all but one products of a distillation unit are varied simultaneously. For a system with more than one distillation unit (e.g., an atmospheric distillation unit and a vacuum distillation unit), the distillation unit to modify is selected at random. The new flow rates are random numbers with values between the lower and upper bounds previously specified by the designer (see section 4.2).

2. **Change a stripping steam flow rate**. This move randomly selects a stripping steam stream and changes its flow rate. The new flow rate is a random number with a value between the specified lower and upper bounds.

3. **Change the feed temperature**. This move randomly selects a feed stream of a distillation unit a modifies its inlet temperature (furnace coil outlet temperature, COT). This temperature may refer, for example, to the crude oil feed leaving the furnace and entering an atmospheric distillation unit or to the atmospheric residue leaving the furnace and entering a vacuum distillation unit. The new feed temperature is randomly selected from the lower and upper bounds specified by the designer.

4. **Change pump-around duties**. In this move, the pump-around duties of a distillation unit are randomly varied along their lower and upper bounds. The mass flow rate and temperature drop specifications are left unchanged.

5. **Change pump-around temperature drops**. Similarly to the "change pump-around duties" move, this move varies the pump-around temperature drops of a distillation unit. The new temperature drops are random numbers with values between the specified lower and upper bounds. The mass flow rate and duty specifications are left unchanged. Pump-around flow rates can be used as optimization variables instead of pump-around duties or temperature drops.

In the approach of Chen,[7] key components of the distillation column and their recoveries are considered as optimization variables. These variables are used as inputs of the FUG-based distillation model. However, these specifications are not as meaningful in the petroleum industry as, for example, product flow rates and their boiling properties (e.g., true boiling point temperatures). Thus, Chen[7] employs an optimization-based procedure to translate product flow rates and TBP points into key components and their recoveries. This procedure is computationally demanding and very sensitive to initial guesses,[20] which leads to convergence failures. Liu[20] proposed a simpler and more robust procedure than the one used by Chen[7] to identify the key components and recoveries. However, the procedure of Liu[20] has not yet been implemented in the distillation system optimization framework and is still most relevant in the context of short-cut models.

Contrary to the approach of Chen,[7] this work directly considers product flow rates and TBP points as variables in the overall optimization framework. Thus, it is not necessary to employ the key component identification procedure of Chen.[7] In this work, product flow rates are considered as inputs of the ANN distillation model, while the product TBP points are predicted (outputs) by the ANN model.

The optimization variables presented in Figure 4 are not an exhaustive list. For example, the reflux ratio at the top of the column could also be included as a CDU move. Such variables would need to be included in the underlying simulation model as independent variables. Part I[2] of the series provides further details on setting up the ANN distillation model.

4.4. Optimization Framework. The design approach presented in this work implements the simulation and retrofit models, the objective function, and constraints into the SA optimization framework. Figure 5 illustrates the optimization-based design approach for the overall distillation system. The procedure is described below:

1. The designer specifies a feasible set of operating conditions and HEN structure. The lower and upper bounds of the optimization variables and the distillation system constraints are also specified, as discussed in section 4.2.

2. The objective function for optimization is selected. In this work, the selected objective function is the maximization of net profit (eq 1). However, other objective functions (e.g., minimize utility consumption, maximize product revenue, etc.) can be used.

3. The tuning parameters of the SA algorithm (e.g., annealing temperature, Markov chain length, number of iterations, etc.)

are specified. In this work, several tests were run to select the values of the SA parameters.

4. The optimizer starts with a feasible set of operating conditions and HEN structure. The objective function for the initial distillation system is calculated.

5. For each iteration, the algorithm randomly selects the SA move to be implemented in the distillation system. Moves related to the CDU are applied according to the description in section 4.3. Moves related to the HEN are applied according to the description in section 4.1.3 of part II.[3]

6. Once the CDU or HEN move is applied, the distillation system is simulated to compute the objective function. The simulation procedure is described in section 3. If the distillation system is feasible, the penalties of the objective function (eqs 4 and 5) are also computed.

7. For a feasible set of operating conditions and HEN structure, the SA algorithm accepts or rejects each design based on the value of the objective function and the SA acceptance criterion. Otherwise, the design is automatically rejected by the optimizer. The Metropolis acceptance criterion[21] is used in this work to decide whether a feasible design is accepted or rejected.

8. Steps 6 and 7 are repeated until the SA termination criterion is met. A description of the SA algorithm and the various termination criteria used in this work is described in part II.[3]

The design problem formulated in this work is a nonlinear and highly combinatorial optimization problem. The HEN retrofit problem is highly combinatorial in nature due to the many combinations of structural arrangements that can be proposed. Nonlinearity is introduced by the use of nonlinear models (e.g., CDU and HEN models, cost models) and constraints.

Although simpler and more robust than rigorous and simplified distillation models, the ANN simulation model used in this work is nonlinear. The main difference between the ANN distillation model and rigorous or simplified models is that the solution of the ANN model equations is straightfor-ward. No initial guesses are required, nor are complex algorithms needed to solve the model equations. The computational burden of using the simplified models of Chen[7] in the optimization framework is overcome by using the ANN distillation model.

The simulation of the HEN is more computationally demanding than the simulation of the CDU (using ANN models). The HEN simulation model is formulated as two systems of linear equations, one for the mass balance and one for the energy balance. If temperature-dependent heat capacities are considered, the energy balance needs to be repeatedly solved to converge one simulation. On the other hand, the HEN feasibility solver is formulated as a nonlinear least-squares problem. This problem is highly nonlinear and very difficult to solve. Multiple HEN simulations are carried out by the feasibility solver to find the duties and split fractions that regain HEN feasibility.

Optimization algorithms used to solve this complex mixed-integer nonlinear programming (MINLP) problem play a very important role. They should be effective and computationally efficient for generating designs and analyzing them. The No Free Lunch Theorems[22] state that no general-purpose universal optimization strategy is possible and imply that optimization algorithms should be chosen depending on the characteristics (e.g., type of objective function, constraints, and variables) of the problem under consideration. This has been taken into account to divide the distillation system design problem into two different types of problems, for which suitable optimization algorithms are used. That is, SA is used to optimize the CDU operating conditions and HEN structure, which is a highly combinatorial nonlinear problem with discrete and continuous variables. As a subproblem, the Levenberg−Marquardt algorithm is employed to recover HEN feasibility, which is a least-squares problem of continuous variables. A discussion of the advantages and limitations of the SA algorithm over deterministic optimization methods is presented in part II[3] of the series.

It can be argued that decomposing the distillation system design problem into two levels can lead to suboptimal solutions.[23,24] However, it would be very time-consuming for the SA algorithm to produce the same quality of results using a single-level formulation. In contrast, if a purely deterministic algorithm was used to formulate a single-level problem, a substantial number of optimization runs with different starting points may be necessary to produce the same quality of solutions due to the inability of deterministic algorithms to escape local minima.

5. CASE STUDIES

The methodology described in this paper is applied in three case studies. In case study 1, an atmospheric distillation unit and the associated HEN are optimized together for net profit improvement. Two different scenarios are explored, namely optimization with and without considering constraints on heat transfer area. The atmospheric distillation unit and HEN presented in case study 1 have been optimized individually in the previous parts of this series.[2,3] However, this paper considers the simultaneous optimization of the distillation process and heat recovery network.

Case studies 2 and 3 present the optimization of a distillation system consisting of an atmospheric and a vacuum distillation unit, and the corresponding heat exchanger network. In case study 2, the heat-integrated distillation system is optimized for net profit improvement. In case study 3, the distillation system is optimized to minimize total annualized costs. The main difference between optimization for net profit improvement and annualized cost reduction is that the former includes the optimization of product yields, while for the latter these yields are fixed.

The SA optimization degrees of freedom for the distillation process include the flow rates of distillation products and stripping steam, pump-around duties and temperature drops, and furnace exit temperature. For the heat exchanger network, SA degrees of freedom include the number and type of structural modifications that can be performed such as adding and removing a heat exchanger, repiping a heat exchanger, etc. For the HEN feasibility solver, the optimization degrees of freedom include the heat loads of heat exchangers and split fractions of stream splitters.

5.1. Case Study 1. The configuration and initial operating conditions of the atmospheric distillation unit and HEN used in this case study have been described in detail in parts I[2] and II,[3] respectively. However, for the sake of completeness, the main information related to the existing distillation system is presented again in this paper. The configuration and initial operating conditions of this distillation system are taken from Chen.[7] The design of the atmospheric distillation unit (ADU) was originally developed by Suphanit[10] following the design guidelines presented by Watkins.[25]
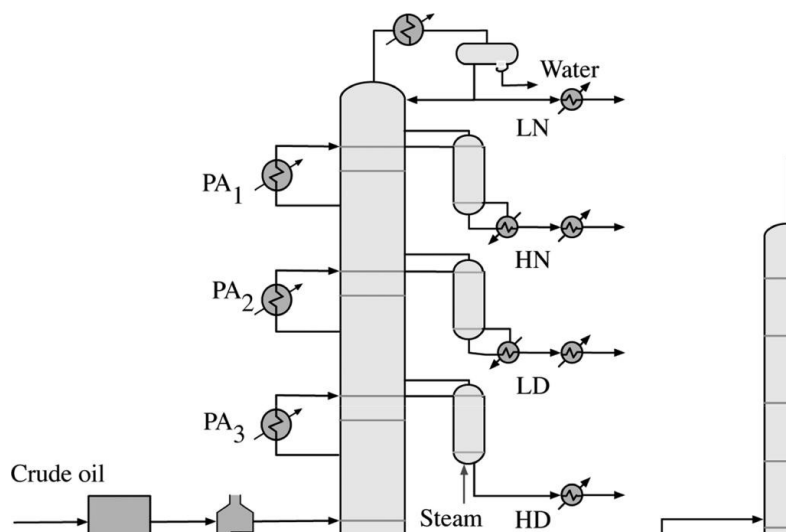
Figure 6. Atmospheric and vacuum distillation units.

The objective of this case study is to maximize net profit by varying the product yields according to their economic value and by reducing the costs of utilities and stripping steam. Two scenarios are considered, namely optimization with and without including constraints on heat transfer area. Retrofit of the HEN is taken into account to accommodate the changes to the operating conditions of the ADU.

5.1.1. Base Case Problem Data. The ADU is configured as a main tower with three side strippers, three pump-arounds and one condenser, as in Figure 6. This ADU processes 100000 bbl/day (0.184 m^3/s) of Venezuela Tia Juana Light Crude[25] to produce five products: light naphtha (LN), heavy naphtha (HN), light distillate (LD), heavy distillate (HD), and residue (RES). Steam is used as a stripping agent for the main column and HD stripper, while reboiling is used for the HN and LD strippers.

The stage distribution of the ADU is presented in Table S1 (see Supporting Information), while Table 2 lists the initial operating conditions. The product flow rates in Table 2 are reported as ideal liquid flow rates at standard conditions (15 °C and 1 atm) on a water-free basis. Tables 3 and 4 show the T5% and T95% TBP temperatures of the distillation products and column flooding percentage at the initial operating conditions, respectively.

Figure 7 illustrates the initial HEN structure. The HEN consists of 13 process-to-process heat exchangers and seven coolers and process furnaces (represented by units 14 and 15). Tables S2 and S3 (see Supporting Information) summarize the HEN specifications. The calculated area is 5754 m^2, which is also considered as the installed heat transfer area. The heat transfer areas of units 14 and 15 are not considered in this case study as the configuration and design equation of a furnace are very different from those of shell and tube heat exchangers, reboilers, or condensers. Thus, it is assumed that the existing furnace accommodates the initial heat transfer area requirements. Fired heating and cooling water are used as hot and cold utilities, respectively. Pressure drops in the heat exchangers are not considered, and heat transfer coefficients are assumed constant for each heat exchanger, even if stream temperatures, flow rates, and properties change.

The minimum temperature approach of the HEN is 25 °C. The hot and cold utility requirements calculated in this work

Table 2. Case Study 1: Optimization Variables of Atmospheric Distillation Unit

item	base case	optimized case	
		case study 1.1	case study 1.2
LN flow rate (bbl/h)	465.9	506.0 (+9%)	416.5 (−11%)
HN flow rate (bbl/h)	483.6	384.8 (−20%)	486.1 (+1%)
LD flow rate (bbl/h)	921.9	957.0 (+4%)	971.2 (+5%)
HD flow rate (bbl/h)	285.7	362.1 (+27%)	329.0 (+15%)
RES flow rate (bbl/h)	2009.6	1956.9 (−3%)	1963.9 (−2%)
PA1 duty (MW)	11.20	10.31 (−8%)	8.00 (−29%)
PA2 duty (MW)	17.89	21.51 (+20%)	17.78 (−1%)
PA3 duty (MW)	12.84	16.61 (+29%)	13.87 (+8%)
PA1 temperature drop (°C)	20.0	19.7 (−2%)	21.9 (+10%)
PA2 temperature drop (°C)	50.0	44.1 (−12%)	39.6 (−21%)
PA3 temperature drop (°C)	30.0	32.4 (+8%)	21.3 (−29%)
RES steam flow rate (kmol/h)	1200.0	1054.8 (−12%)	1199.6 (~0%)
HD steam flow rate (kmol/h)	250.0	176.1 (−30%)	201.7 (−19%)
coil outlet temperature (°C)	365.0	362.7 (−2 °C)	365.0 (~0 °C)

Table 3. Case Study 1: Product Quality Results

item	base case	optimized case	
		case study 1.1	case study 1.2
LN T5% (°C)	6	6 (+1)	5 (−1)
HN T5% (°C)	102	99 (−2)	93 (−9)
LD T5% (°C)	174	169 (−5)	170 (−4)
HD T5% (°C)	289	284 (−5)	289 (−1)
RES T5% (°C)	358	364 (+6)	364 (+6)
LN T95% (°C)	111	115 (+4)	109 (−2)
HN T95% (°C)	187	185 (−2)	184 (−3)
LD T95% (°C)	312	311 (−1)	312 (~0)
HD T95% (°C)	363	366 (+3)	365 (+2)
RES T95% (°C)	889	893 (+4)	892 (+3)

for the initial distillation system are 60.82 MW and 67.05 MW. For the same ADU operating conditions and HEN structure, Chen[7] reports hot and cold utility requirements equal to 63.80

Table 4. Case Study 1: Column Flooding Percentage for the
Atmospheric Distillation Unit

		optimized case	
	base		case study
section	case	case study 1.1	1.2
main column stages 1−5	36	33	35
main column stages 6−14	52	46	50
main column stages 15−24	68	64	73
main column stages 25−32	75	70	77
main column stages 33−41	84	67	76
HD stripper	21	20	21
LD stripper	47	48	49
HN stripper	32	26	32

MW and 67.26 MW. This represents a difference of 2.98 MW
and 0.21 MW from the values reported in this work. Calculated
heat transfer areas and heat loads are also different. These
discrepancies may be explained by the prediction errors of
simplified models[7] and ANN models[2] when compared to
results from rigorous simulations. Table S2 (see Supporting
Information) shows the prediction errors of the stream
information used to simulate the HEN.

Simplified models present errors greater than 20 °C for the
supply temperatures of pump-arounds 1 and 2, while the supply
and target temperatures of the reboilers present errors greater
than 10 °C. Enthalpy change prediction errors for simplified
models are as high as 81% for the HN reboiler stream. On the
other hand, prediction errors of supply and target temperatures
with the ANN distillation model are below 1 °C for all streams,
while enthalpy change prediction errors are below 1%
compared to rigorous model predictions. These differences in
stream data of simplified models and ANN models make it
necessary to recalculate heat loads and heat transfer areas of the
original HEN design proposed by Chen.[7]

The prices of the distillation products are presented in Table
1. The prices of stripping steam and utilities and the exchanger
modification costs are listed in Table S4 (see Supporting
Information). The cost of utilities and stripping steam is 11.2 M
$/y (millions of US $ per year), while the cost of crude oil is
2852.3 M$/y. The estimated product revenue is 2881.9 M$/y,
thus the net profit is 18.3 M$/y.

5.1.2. Objective Function, Variables, And Constraints. The
objective function of this case study is to maximize net profit,
i.e., maximize eq 1. Two scenarios are explored: the first
scenario (referred to as case study 1.1) does not consider
constraints on heat transfer area; in the second scenario (case
study 1.2), these constraints are active. The optimization
degrees of freedom of the ADU are listed in Table 2. Note that
the flow rate of the RES stream is not an optimization variable
and is calculated as the flow rate of crude oil less the flow rates
of LN, HN, LD, and HD products. These optimization
variables (except for the coil outlet temperature) are con-
strained to vary ±30% from their base case values. For the coil
outlet temperature, the lower and upper bounds are 330 °C and
370 °C, respectively. The T5% and T95% TBP temperature
specifications for products are allowed to vary no more than

±10 °C from the base case values. Column flooding percentage

is constrained to be below 85%.

Regarding the constraints on the HEN topology, the

maximum number of new heat exchangers and splitters is

two; only one heat exchanger may be removed, and one

resequencing and one repiping modification is permitted. The

total annualized cost of the distillation system is calculated
assuming a 2-year project life with a 5% interest rate, and an

operating time of 8600 h per year. For case study 1.2, the lower

bound for the calculated heat transfer areas is 10 m^2; the lower

and upper bounds for additional heat transfer areas are equal to

10% and 40% of the installed areas. Note that it is possible to

assign different values for the constraints from those considered

in this case study to constrain the heat transfer areas of each

heat exchanger.

5.1.3. Optimization Approach. The ANN model employed

to simulate the ADU is the one developed in part I,[2] together

with the equations used to estimate the temperature-dependent

heat capacity flow rates described in part II.[3] The HEN retrofit
and simulation models are those presented in part II.[3] The

simulation model for the ADU and HEN are implemented as

described in section 3. The HEN retrofit model is implemented
in the optimization framework as described in section 4.3.

Table 5 presents the move probabilities used in case study 1.

The values of these probabilities were selected by considering

that changes to the operating conditions of the ADU have a
dominant effect on the system's economics. Particularly for this

Figure 7. Case study 1: structure of existing heat exchanger network.

Table 7. Case Study 1: Heat Transfer Areas for Base Case and Optimized Cases with and without Considering Constraints on Heat Transfer Area

	calculated areas (m^2)		
exchanger no.	base case	case study 1.1	case study 1.2
1	1018	868 (−15%)	935 (−8%)
2	808	1311 (+62%)	985 (+22%)
3	110	213 (+93%)	121 (+10%)
4	298	397 (+33%)	418 (+40%)
5	95	108 (+14%)	85 (−11%)
6	117	275 (+135%)	55 (−53%)
7	465	726 (+56%)	465 (~0%)
8	255		280 (+10%)
9	347	287 (−17%)	379 (+10%)
10	78	47 (−40%)	110 (+40%)
11	558	786 (+41%)	638 (+14%)
12	23	10 (−57%)	10 (−55%)
13	10	10 (−1%)	11 (+10%)
14^{HU}			
15^{HU}			
17^{CU}	48	53 (+12%)	41 (−14%)
18^{CU}	71	96 (+34%)	37 (−48%)
19^{CU}	103	83 (−20%)	101 (−2%)
20^{CU}	48	73 (+52%)	53 (+10%)
21^{CU}	1169	852 (−27%)	1287 (+10%)
22^{CU}	122	92 (−25%)	134 (+10%)
24^{CU}	10	19 (+92%)	11 (+10%)
25		59	
total area	5754	6365 (+11%)	6157 (+7%)
additional area		1428	615
new HE area		59	

of 1487 m^2. Table 7 shows that the required heat transfer areas of units 3 and 24 almost double their installed areas, while the required heat transfer area for unit 6 is around 135% greater than its installed area. Section S1.2 (see Supporting Information) presents the optimized input specifications for HEN simulation (supply and target temperatures, stream enthalpy changes, stream heat capacity ratios, heat exchanger heat loads, and heat transfer coefficients) and the HEN

simulation results (stream temperatures, heat transfer areas, and LMTDs).

5.1.5. Results for Case Study 1.2. In this scenario, additional heat transfer areas are constrained. The lower and upper bounds for these variables are equal to 10% and 40% of the installed area. The lower bound for the calculated heat transfer area of each heat exchanger is 10 m^2.

The optimized operating conditions of the ADU are presented in Table 2. Table 6 summarizes the economic results for these optimized operating conditions. Net profit increased by 12 M$/y, about half of that for case study 1.1. As expected, product revenue is the main factor affecting the improvement of net profit. Product revenue is increased by 11.8 M$/y, while the TAC is marginally reduced. The flow rates of the HN, LD and HD products are increased by 2, 49, and 43 bbl/h, respectively; the flow rates of the LN and RES products are reduced by 49 and 46 bbl/h. Product quality is kept within specifications, as shown in Table 3. The column flooding percentage meets constraints (Table 4).

The hot and cold utility requirements are decreased by only 1.26 MW and 0.90 MW, which is equivalent to a reduction of 2% and 1% from the initial requirements. This reduction in utility consumption is substantially less attractive than that of case study 1.1. The same effect is observed for the consumption of stripping steam.

The required capital investment for case study 1.2 (0.2 M$) is less than half of that of case study 1.1 (0.40 M$). The reason for this is that the HEN of case study 1.2 does not have any topology changes; that is, its configuration is the same as that of the base case (see Figure 7). Another reason is that the constraints imposed to the maximum additional area of each heat exchanger limit the costs of adding new area to the HEN. However, although more conservative values for additional area are obtained in case study 1.2, the disadvantage is that only marginal savings in operating costs are achieved. From these results, it can be inferred that constraints on heat transfer areas restrict the operational optimization of the ADU as well as the topology modifications that can be made to the HEN.

5.2. Case Study 2. The objective of this case study is to improve the net profit of a distillation system consisting of an atmospheric distillation unit, a vacuum distillation unit, and the
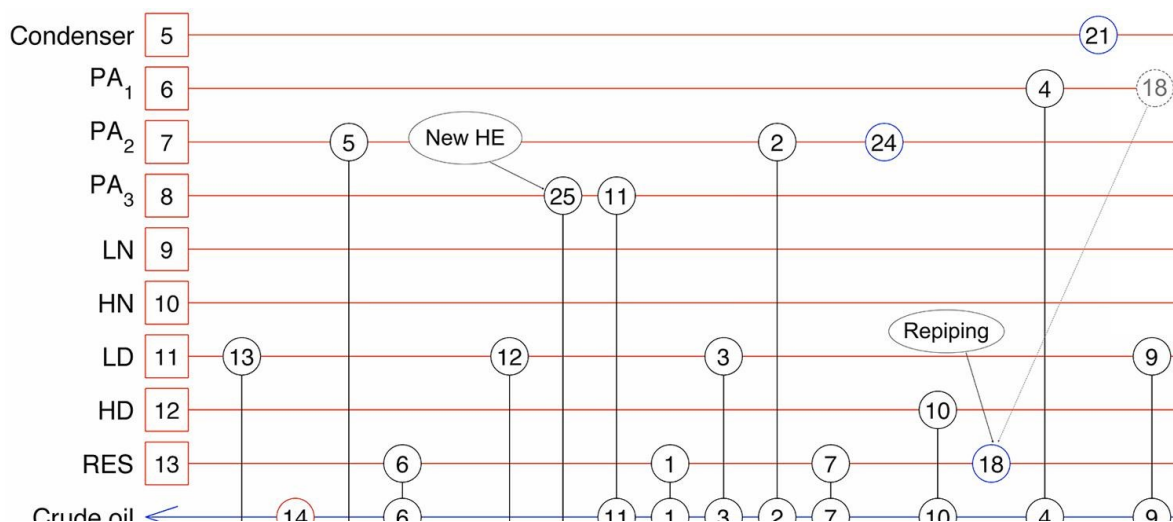
Figure 8. Case study 1.1: proposed retrofit modifications. Unconstrained area.

L

associated heat exchanger network, as illustrated in Figure 6. The optimization degrees of freedom include the yields of the distillation products, pump-around duties and temperature drops, stripping steam flow rates and furnace exit temperatures. HEN retrofit is considered.

The initial crude oil distillation system is taken from Chen.[7] The design of the ADU was originally developed by Suphanit,[10] while the design of the vacuum distillation unit (VDU) was developed by Rastogi.[12] The designs of both distillation units were carried out following the design guidelines presented by Watkins.[25]

5.2.1. Base Case Problem Data. The distillation system processes 100,000 bbl/day (0.184 m³/s) of Venezuela Tia Juana Light Crude.[25] The crude oil enters the ADU and is fractionated into five products: LN, HN, LD, HD, and RES. The RES stream from the ADU is heated in a furnace before entering the VDU. The VDU produces four products, namely vapor (VAP), light vacuum gas oil (LVGO), heavy vacuum gas oil (HVGO), and vacuum residue (VRES). The configuration and stage distribution of the ADU are the same as in case study 1, although the operating pressures are different. Table S12 (see Supporting Information) presents the pressure specifications for the ADU. The VDU is configured as a main column with two pump-arounds. The operating pressures of the VDU are listed in Table S12 (see Supporting Information); the stage distribution and column diameters are presented in Table S13 (see Supporting Information).

The initial operating conditions of the distillation units are shown in Table 8. Table 9 presents the T5% and T95% TBP temperatures of the distillation products. Table 10 lists the column flooding percentage for the different column sections of the distillation units.

The existing HEN is presented in Figure 9. The HEN consists of 18 process-to-process heat exchangers, eight coolers, three heaters, and two stream splitters. The minimum temperature approach of the HEN is 25 °C. Fired heating and cooling water are used as hot and cold utilities. Pressure drops in the heat exchangers are not considered, and heat transfer coefficients are assumed constant.

As in case study 1, the heat loads, split fractions, and heat transfer areas of the initial HEN need to be recalculated as a result of the differences between the stream information provided by Chen[7] and the predictions of the ANN distillation models used in this work. Table S18 (see Supporting Information shows the prediction errors of simplified models and ANN distillation models when compared to rigorous models. For simplified models, errors in the temperatures of PA₁, PA₂, and PA₄ are greater than 25 °C, while the errors for the reboiler streams and HN, LD, LVGO, and VRES products are close to 20 °C. Substantial differences are also found for the prediction of enthalpy changes using simplified models. In contrast, prediction errors of the ANN models for temperature-related variables is less or equal than 1 °C, while the errors for most of the enthalpy predictions are below 3%. These results demonstrate that ANN distillation models can be considerably more accurate than simplified models.

The split fractions in the initial HEN are 0.88 (to HE 28) and 0.51 (to HE 13). The current hot and cold utility requirements are 83.07 MW and 97.22 MW, respectively. The details of the HEN are presented in section S2.4 (see Supporting Information), including heat loads, heat transfer areas, heat transfer coefficients, LMTDs, and stream temper-

Table 8. Case Studies 2 and 3: Optimization Variables of Crude Oil Distillation Units

item	base case	optimized case	
		case study 2	case study 3
Atmospheric Unit			
LN flow rate (bbl/h)	471.0	501.3 (+6%)	471.0
HN flow rate (bbl/h)	480.0	436.6 (−9%)	480.0
LD flow rate (bbl/h)	919.7	934.2 (+2%)	919.7
HD flow rate (bbl/h)	294.5	347.0 (+18%)	294.5
RES flow rate (bbl/h)	2001.5	1947.6 (−3%)	2001.5
PA₁ duty (MW)	9.64	10.82 (+12%)	7.92 (−18%)
PA₂ duty (MW)	18.69	21.84 (+17%)	22.62 (+21%)
PA₃ duty (MW)	13.14	13.65 (+4%)	13.90 (+6%)
PA₁ temperature drop (°C)	20.0	15.2 (−24%)	25.4 (+27%)
PA₂ temperature drop (°C)	50.0	49.1 (−2%)	45.2 (−10%)
PA₃ temperature drop (°C)	30.0	33.8 (+13%)	30.0 (0%)
RES steam flow rate (kmol/h)	1200.0	1153.5 (−4%)	1200.0 (0%)
HD steam flow rate (kmol/h)	250.0	186.9 (−25%)	250.0 (0%)
coil outlet temperature (°C)	365.0	358.0 (−7 °C)	344.3 (−21 °C)
Vacuum Unit			
VAP flow rate (bbl/h)	105.6	63.0 (−40%)	105.6
LVGO flow rate (bbl/h)	235.8	241.3 (+2%)	235.8
HVGO flow rate (bbl/h)	667.7	685.2 (+3%)	667.7
VRES flow rate (bbl/h)	992.4	958.1 (−3%)	992.4
PA₄ duty (MW)	11.3	11.4 (~0%)	13.4 (+18%)
PA₅ duty (MW)	16.0	18.3 (+14%)	19.8 (+24%)
PA₄ temperature drop (°C)	100.0	103.3 (+3%)	77.5 (−23%)
PA₅ temperature drop (°C)	150.0	105.8 (−29%)	127.7 (−15%)
VRES steam flow rate (kmol/h)	700.0	700.0 (~0%)	569.0 (−19%)
coil outlet temperature (°C)	400	362.1 (−38 °C)	351.08 (−49 °C)

Table 9. Case Studies 2 and 3: Product Quality Results

item	base case	optimized case	
		case study 2	case study 3
LN T5% (°C)	6	6 (+1)	6 (~0)
HN T5% (°C)	107	108 (+2)	105 (−2)
LD T5% (°C)	181	173 (−8)	174 (−7)
HD T5% (°C)	290	289 (−1)	287 (−3)
RES T5% (°C)	359	365 (+6)	359 (−1)
LVGO T5% (°C)	342	343 (+1)	340 (−2)
HVGO T5% (°C)	374	378 (+3)	376 (+1)
VRES T5% (°C)	505	509 (+4)	506 (+1)
LN T95% (°C)	111	112 (+1)	111 (~0)
HN T95% (°C)	187	187 (~0)	187 (~0)
LD T95% (°C)	312	312 (~0)	312 (~0)
HD T95% (°C)	363	367 (+4)	364 (+1)
RES T95% (°C)	890	894 (+4)	890 (~0)
LVGO T95% (°C)	452	455 (+3)	453 (+1)
HVGO T95% (°C)	511	512 (~0)	510 (−1)
VRES T95% (°C)	982	986 (+4)	982 (~0)

atures. The stream data (supply and target temperatures,

Table 10. Case Studies 2 and 3: Column Flooding Percentage for the Atmospheric and Vacuum Distillation Units

		optimized case	
section	base case	case study 2	case study 3
Atmospheric Unit			
main column stages 1−5	36	33	33
main column stages 6−14	56	49	45
main column stages 15−24	72	65	61
main column stages 25−32	85	80	74
main column stages 33−41	94	90	65
HD stripper	23	21	21
LD stripper	49	50	49
HN stripper	36	33	36
Vacuum Unit			
stages 1−3	46	44	49
stages 4−5	45	48	51
stages 6−7	40	43	46
stages 8−9	40	60	69

stream enthalpy changes, and heat capacity flow rate ratios) for the initial HEN are also presented in section S2.4 (see Supporting Information). The equations used to estimate the temperature-dependent heat capacity flow rates of the process streams are described in section S2.3 (see Supporting Information).

The prices and crude oil and distillation products are the same as in case study 1 except for the price of the RES stream. In this case, the price of the RES product was changed to 61.4 $/bbl to account for the operating costs of the VDU. The prices of stripping steam, utilities, and HEN retrofit costs are the same as in case study 1 (see Table S4 in Supporting Information). The project life is two years, with an interest rate of 5% and an operating time of 8600 h/y. Utilities cost 13.0 M

$/y, stripping steam costs are 2.6 M$/y, product revenue is 2,886.2 M$/y, and the current net profit is 18.3 M$/y.

5.2.2. Objective Function, Variables, and Constraints. The objective function for this case study is to maximize the net profit (i.e., eq 1). The optimization degrees of freedom of the distillation units are listed in Table 8. Note that the flow rates of the RES and VAP products are dependent variables not optimization variables. The optimization degrees of freedom of the HEN include the different structural modifications that can be performed and are listed in Figure 4.

The optimization variables listed in Table 8 (except for the coil outlet temperatures) are bounded to values equal to ±30% of the base case values. The lower and upper limits for the coil outlet temperature of the ADU are 330 °C and 370 °C, while for the VDU these values are 350 °C and 410 °C. The T5% and T95% TBP specifications are allowed to vary no more than ±10 °C of the base case values. The column flooding percentage should remain below 90%. The constraints on the topology and heat transfer areas of the heat exchanger network are the same as in case study 1.1. The structures (e.g., stage distribution, column diameters, operating pressures) of the ADU and VDU are not changed during optimization.

5.2.3. Distillation Model and Optimization Approach. The simulation models for the ADU and VDU were developed using the modeling approach described in part I[2] of the series. The information related to the distillation units is used to set up a rigorous simulation in Aspen HYSYS (V7.3).[28] Five thousand randomly generated points were simulated with the rigorous models to produce the data to regress the ANNs. Section S2.2 (see Supporting Information) presents the details of the ANN distillation models, including inputs, outputs, and the architecture of each ANN. The Neural Network Toolbox embedded in MATLAB[13] was used to obtain the ANN distillation models.

The resulting ANN models for the ADU and VDU are implemented in the overall simulation model as described in
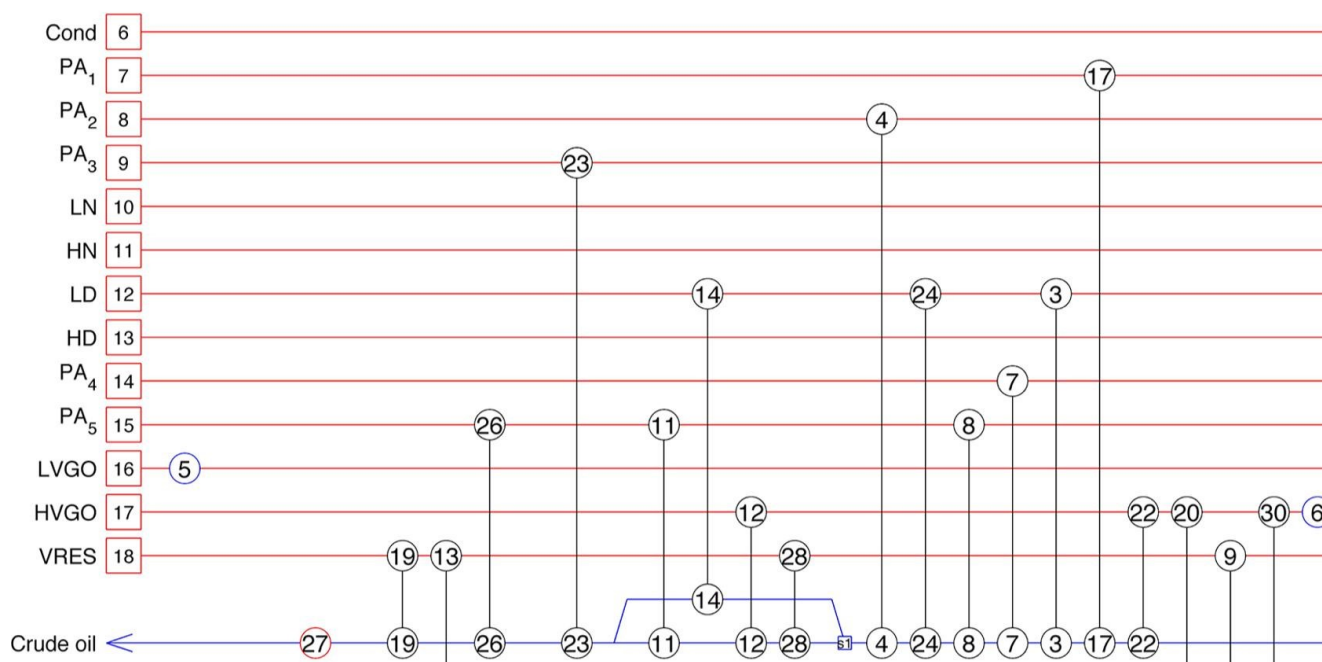
Figure 9. Case study 2: structure of existing heat exchanger network.

section 3. The optimization framework presented in section 4 is employed to maximize eq 1. The same criteria as in case study 1 are used to select the move probabilities of the SA algorithm. The move probabilities related to the distillation units are shown in Table 11. The move probabilities related to the HEN

Table 11. Case Studies 2 and 3: Move Probabilities

move decisions	probability
CDU move; HEN move	0.8; 0.2
ADU move; VDU move	0.5; 0.5
ADU move: product flow rates move; stripping steam flow rate move; feed temperature move; pump-around move	case study 2: 0.8; 0.04; 0.04; 0.12 case study 3: 0.0; 0.2; 0.2; 0.6
ADU pump-around moves: pump-around duties move; pump-around temperature drops move	0.5; 0.5
VDU move: product flow rates move; stripping steam flow rate move; feed temperature move; pump-around move	case study 2: 0.67; 0.07; 0.07; 0.2 case study 3: 0.0; 0.2; 0.2; 0.6
VDU pump-around moves: pump-around duties move; pump-around temperature drops move	0.5; 0.5

are those shown in Table 5. The values of the parameters of the SA algorithm are the same as in case study 1 and are listed in Table S5 (see Supporting Information). Tests were carried out to verify that such values were suitable for the selected objective function. A total of 15 optimization runs were carried out, each run taking approximately 15 min on the same computer as in case study 1. The best design was selected from these runs.

5.2.4. Optimization Results. The optimized operating conditions of the ADU and VDU are presented in Table 8. The product quality results and column flooding percentage at these optimized conditions are shown in Tables 9 and 10, respectively. The optimized HEN structure is illustrated in Figure 10. The details of this HEN (e.g., stream information, heat loads, heat transfer areas, stream temperatures, etc.) are presented in section S2.5 (see Supporting Information).

Table 12 summarizes the results of the best solution in terms of net profit and compares it with the base case costs. The net profit of the distillation system is increased by 24.2 M\$/y compared to the base case. Similar to case study 1, the main contribution of this increase is the improvement of product revenue. Product revenue is increased by 19.9 M\$/y and operating costs are reduced by 4.5 M\$/y, while the required capital investment is approximately 0.4 M\$. The utility costs are reduced by around 4.5 M\$/y, which represents a 35% reduction from the base case costs. Stripping steam costs are reduced by 5% compared to the base case.

Similar to case study 1.1, the optimizer varied the flow rates of the distillation products based on their commercial importance, while considering the feasibility of the distillation system. The flow rates of LN, LD, and HD were increased by 30.3, 14.5, and 52.5 bbl/h, respectively, while the flow rates of HN and RES were decreased by 43.4 and 53.8 bbl/h. The variables related to product quality, namely the T5% and T95% TBP temperatures, are kept within specifications, as shown in Table 9. Table 10 shows that the column flooding percentage in the distillation units is maintained equal or below the maximum permitted value of 90%.

The hot and cold utility consumption is reduced by 28.81 MW (35%) and 15.22 MW (16%), respectively. The main causes for the reduction in hot utility requirements are the increased pump-around duties, the decrease in the target temperatures of the crude oil and RES streams (COTs), and the increase in the crude oil temperature before entering the furnace. Table 8 shows that the COT of the crude oil feed decreases by 7 °C, while the COT for the RES stream decreases by 38 °C compared to the base case. Table S23 (see Supporting Information) shows that the crude oil temperature before entering the furnace rises from 254 °C to 282 °C (28 °C). The total heating requirements of these streams with the optimized target temperatures are reduced by around 14.1 MW, as seen in Table S21 (see Supporting Information). The total duty of the
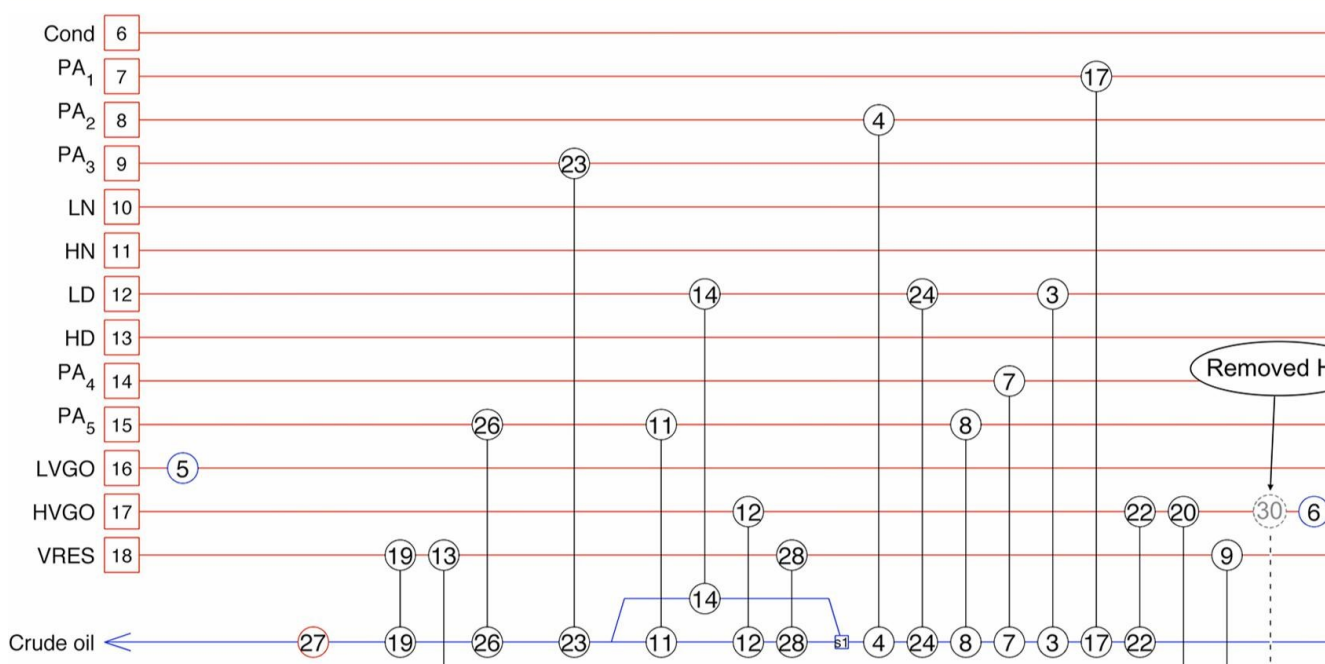
Figure 10. Case study 2: proposed retrofit modifications for net profit improvement.

Table 12. Case Studies 2 and 3: Optimization Results

item	base case	case study 2	case study 3
Utility Consumption			
hot utility (MW)	83.07	54.26 (−35%)	49.16 (−41%)
cold utility (MW)	97.22	82.00 (−16%)	85.52 (−12%)
Operating Costs			
hot utility (M$/y)	12.5	8.1 (−35%)	7.4 (−41%)
cold utility (M$/y)	0.5	0.4 (−16%)	0.4 (−12%)
stripping steam (M$/y)	2.6	2.5 (−5%)	2.4 (−6%)
crude oil (M$/y)	2852.3	2852.3	2852.3
total operating cost (M$/y)	2867.9	2863.4 (~0%)	2862.6 (~0%)
Capital Costs			
new HE area ($)			
additional area ($)		441315	280042
repiping ($)			
resequencing ($)			
total capital costs ($)		441315	280042
ACC ($/y)		237341	150613
Summary			
product revenue (M$/y)	2886.2	2906.1 (+0.4%)	2886.2
TAC ($M/y)	2867.9	2863.6 (~0%)	2862.7 (~0%)
net profit (M$/y)	18.3	42.5 (+24.2 M$/y)	23.5 (+5.2 M$/y)

pump-arounds increases by approximately 7.2 MW. This heat is transferred to the crude oil, which contributes to reducing the hot utility demand. These results indicate that utility costs can be significantly improved when changes to the operating conditions of the distillation process are considered, compared to optimizing the HEN alone (using fixed stream data).

The reduction of cold utility consumption is mainly caused by a reduction in the condenser duty and the increased heat recovery between the VRES and crude oil streams. The condenser duty is reduced by 10.47 MW, compared to the base case, while the cold utility requirements for the VRES decrease by 6.78 MW.

The calculated heat transfer area is 8057 m^2, of which 1937 m^2 correspond to additional area. Table S22 (see Supporting Information) lists the heat transfer areas of each heat exchanger. Two structural modifications are proposed by the SA algorithm, namely removing heat exchanger 30 and removing the stream splitter initially located in the LD reboiler stream. Figure 10 shows these modifications.

This case study shows that the proposed optimization approach is able to produce cost-effective designs for very complex crude oil distillation systems. The optimizer achieved a substantial increase in product revenue as well as a considerable reduction in operating costs. Product quality was maintained for the improved product yields. The retrofitted HEN presents a reasonable number of structural modifications, with a relatively low capital investment required. Note that 16 heat exchangers need additional area in the new HEN design, which may pose a challenge when implementing these modifications in a single shut-down, with limited time.

5.3. Case Study 3. The objective of this case study is to decrease the total annualized cost of the same existing crude oil distillation system presented in case study 2 (Section 5.2). The total annualized cost is defined in this work as the sum of operating costs (eq 2) and the annualized capital investment required to retrofit the HEN. Product yields are fixed in this case study.

5.3.1. Base Case Problem Data. The details of the existing distillation units are described in section 5.2.1. The

configuration of the distillation units is presented in Tables S1 and S13 (see Supporting Information), the pressure specifications in Table S12 (see Supporting Information), the operating conditions in Table 8, the T5% and T95% TBP specifications in Table 9, and flooding percentage for the various column sections in Table 10.

The same heat exchanger network presented in case study 2 is used in this case study. The grid diagram of the initial HEN is shown in Figure 9. The stream information used to simulate the HEN is presented in Table S17 (see Supporting Information). The breakdown of heat loads, heat transfer coefficients, heat transfer areas, and stream temperatures is listed in Tables S19 and S20 (see Supporting Information).

The prices of the distillation products and utilities and cost of HEN modifications are the same as in case study 2. The total annualized cost for the initial distillation system is 2867.9 M $/y, of which 13.0 M$/y corresponds to utility costs, 2.6 M$/y to stripping steam cost, and 2852.3 M$/y to the crude oil cost. The cost of crude oil is fixed because the flow rate of this stream does not change.

5.3.2. Objective Function, Variables, And Constraints. The objective function of this case study is to minimize the total annualized cost of the distillation system. The optimization variables for the ADU and VDU are the pump-around duties and temperature drops, the flow rates of stripping steam streams, and the coil outlet temperatures. The flow rates of the distillation products are fixed. The optimization variables for the HEN are the same as in case study 2 and are shown in Figure 4.

The constraints considered in this case study are the same as in case study 2. Section 5.2.2 describes the constraints on the operating conditions of the distillation units, product quality, column flooding percentage, and modifications that can be made to the HEN. The structure of the distillation units is not changed.

5.3.3. Distillation Model, Optimization Approach. The distillation models developed in case study 2 are also used in this example. The move probabilities for the distillation units are presented in Table 11, while Table 5 shows the probabilities
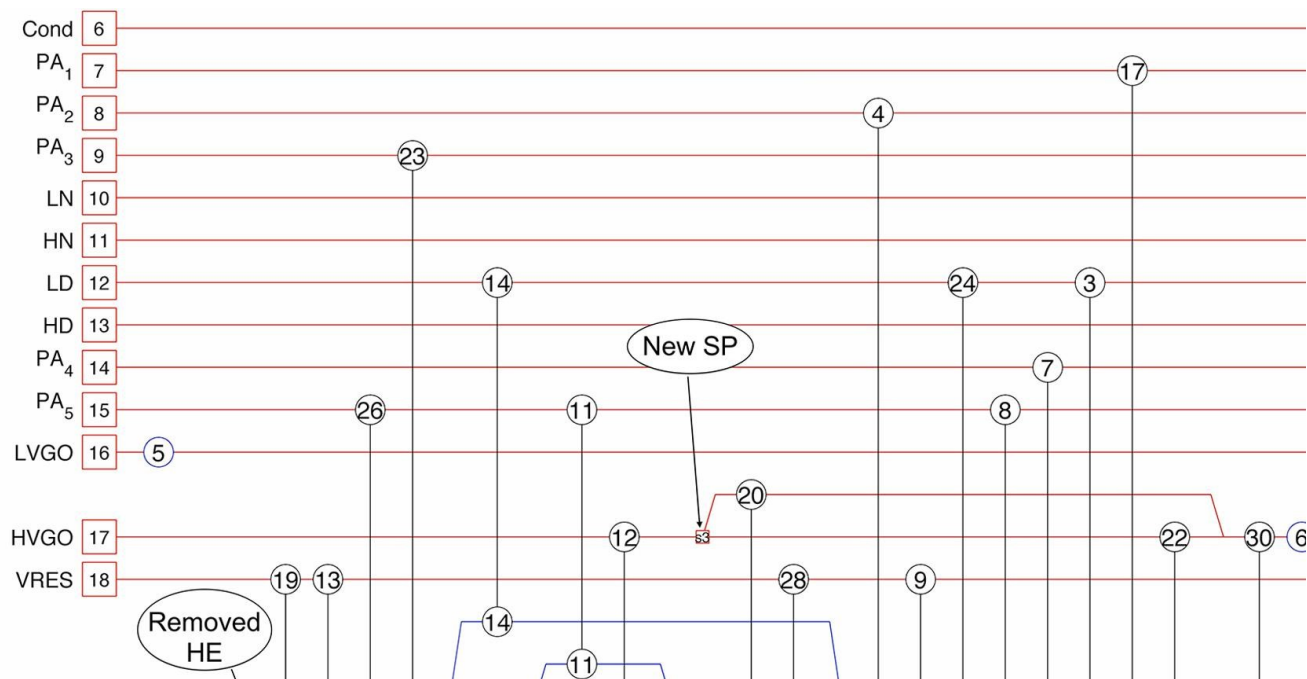
Figure 11. Case study 3: proposed retrofit modifications for annualized cost reduction.

for the HEN. A probability equal to zero is assigned to the "change the product flow rates" moves to forbid changes to product yields.

The multiple-run simulated annealing-based design frame-work is applied to minimize the total annualized cost of the distillation system. The simulated annealing parameters implemented in the optimization are presented in Table S5 (see Supporting Information).

5.3.4. Optimization Results. Table 12 presents the summary of the best solution found during the optimization and compares it with the base case. Table 8 shows the values of the optimization variables and their relative changes from the base case. The results for the variables related to product quality and column flooding are presented in Tables 9 and 10. The grid diagram of the optimized HEN is shown in Figure 11. The details of this HEN are presented in section S3 (see Supporting Information).

Even though the flow rates of the distillation products remain fixed, the T5% and T95% TBP temperatures change, especially for the T5% TBP temperature of the LD stream. However, product quality for all products is kept within specifications, as shown in Table 9. The constraints on the column flooding percentage are not violated (Table 10).

The hot and cold utility requirements are reduced by 33.91 MW (41%) and 11.70 MW (12%), respectively. This represents a reduction of 5.2 M$/y (40%) in utility costs. The total flow rate of stripping steam is reduced by 6%, which represents a cost reduction of approximately 0.2 M$/y.

Similar to case study 2, the duties of the pump-arounds 2−5 are increased to improve energy recovery, while the coil outlet temperatures of the crude oil and RES streams are decreased to reduce overall heating requirements. The COTs of the crude oil and RES streams are reduced by 21 °C and 49 °C, respectively. This represents a reduction in heating requirements of 21.54 MW. The temperature of the crude oil before entering the furnace is changed from 254 °C to 269 °C (15 °C) as a result

of the increased energy recovery between the process streams. These temperature changes contribute to a substantial reduction in the hot utility consumption. The condenser duty was reduced by 11.84 MW, decreasing the cold utility consumption. Tables S17 and S24 (see Supporting Information)) show the enthalpy changes for these streams at the base case and optimized conditions. From these results, it can be concluded that changes to the operating conditions of the ADU and VDU have a significant effect on the operating costs related to the heat exchanger network.

The retrofit modifications for the HEN are shown in Figure 11. These modifications include removing exchanger 10 and adding two stream splitters, one in the crude oil feed and the other in the HVGO stream. The calculated heat transfer area is 7434 m², of which 1190 m² correspond to additional area. Table S25 (see Supporting Information) list the heat transfer areas of each exchanger. The capital investment required to implement these modifications is around 0.3 M$. This amount is significantly less than the reduction in operating costs.

6. CONCLUSIONS

This paper presents a new approach to optimize heat-integrated crude oil distillation systems. The main features of this approach are the simultaneous consideration of the distillation process and HEN in the optimization framework and the consideration of practical constraints related to the distillation process (e.g., product quality, column flooding) and HEN (HEN topology, heat transfer area, etc.). The optimization framework proposed in this work can be applied for different objective functions such as maximizing net profit, minimizing total annualized costs, or minimizing operating costs.

In the proposed approach, the distillation process and HEN are optimized together. A simulation model was developed to capture the synergy between the crude oil distillation unit(s) and the associated heat exchanger network. As a result, the trade-offs within this system are exploited to produce designs

that are not only energy-efficient but that are also able to achieve the desired separation.

The ANN-based modeling approach presented in part I[2] was applied to model the distillation process, while the retrofit and simulation models for the HEN were the ones described in part II[3] of this series. The ANN distillation models used in this work are in very good agreement with rigorous models, are robust, and are computationally efficient. One of the advantages of HEN simulation model is that the topology of the HEN is explicitly addressed in the model equations. This feature of the model facilitates the implementation of topology modifications proposed by the optimizer. Another advantage is that models for temperature-dependent thermal properties can be easily implemented in the HEN simulation model. As for the HEN retrofit model, the main strength is that the designer is able to specify constraints for the number and type of topology modifications and heat transfer areas. This allows more practicable designs to be obtained because issues such as plant layout and safety can be taken into account.

The case studies presented in this paper illustrate the application of the proposed methodology. In these case studies, the operating conditions of the distillation unit(s) are optimized while proposing retrofit modifications to the HEN. The case studies show that product revenue has a dominant influence on net profit, followed by utility costs, stripping steam costs, and capital investment. Results of these case studies also indicate that changes to the coil outlet temperature and pump-around specifications have a major influence on heat recovery. Finally, the case studies show that optimizing the distillation process and HEN together produces more practicable and more economically attractive designs compared to optimizing the distillation process and HEN separately.

Future work related to the distillation process includes the implementation of a model that considers the structural variables of the distillation unit (e.g., location of pump-around and crude oil feed, installation of preflash units, etc.) and the consideration of crude oil blending as an optimization variable. For the heat exchanger network, future work includes the calculation of furnace heat transfer areas, the consideration of fouling and pressure drops in heat exchangers, and the consideration of additional temperature-dependent properties (e.g., density, flow rates, etc.).

■ ASSOCIATED CONTENT

* Supporting Information

Additional data and results for the crude oil distillation systems presented in the case studies. This material is available free of charge via the Internet at http://pubs.acs.org.

■ AUTHOR INFORMATION

Corresponding Author

*Tel: +44 (0) 161 306 6000. E-mail: megan.jobson@manchester.ac.uk.

Notes

The authors declare no competing financial interest.

■ ACKNOWLEDGMENTS

■ REFERENCES

(1) Szklo, A.; Schaeffer, R. Fuel specification, energy consumption and CO2 emission in oil refineries. Energy 2007, 32, 1075−1092 DOI: 10.1016/j.energy.2006.08.008.

(2) Ochoa-Estopier, L. M., Jobson, M., Smith, R. Optimization of Heat-Integrated Crude Oil Distillation Systems. Part I: The Distillation Model. Ind. Eng. Chem. Res. 2015, DOI: 10.1021/ie503802j.

(3) Ochoa-Estopier, L. M., Jobson, M., Chen, L., Rodriguez, C., Smith, R. Optimization of Heat-Integrated Crude Oil Distillation Systems. Part II: Heat Exchanger Network Retrofit Model. Ind. Eng. Chem. Res. 2015, DOI: 10.1021/ie503804u.

(4) Liebmann, K. Integrated Crude Oil Distillation Design. Ph.D. Thesis. University of Manchester Institute of Science and Technology, Manchester, UK, 1996.

(5) Sharma, R.; Jindal, A.; Mandawala, D.; Jana, S. Design/Retrofit Targets of Pump-Around Refluxes for Better Energy Integration of a Crude Distillation Column. Ind. Eng. Chem. Res. 1999, 38, 2411−2417 DOI: 10.1021/ie9802156.

(6) Zhang, J.; Zhu, X. X. Simultaneous Optimization Approach for Heat Exchanger Network Retrofit with Process Changes. Ind. Eng. Chem. Res. 2000, 39, 4963−4973 DOI: 10.1021/ie990634i.

(7) Chen, L. Heat-Integrated Crude Oil Distillation Design. Ph.D. Thesis. The University of Manchester, Manchester, UK, 2008.

(8) Lopez C., D. C.; Hoyos, L. J.; Mahecha, C. A.; Arellano-García, H.; Wozny, G. Optimization Model of Crude Oil Distillation Units for an Optimal Crude Oil Blending and Operating Conditions. Ind. Eng. Chem. Res. 2013, 52, 12993−13005 DOI: 10.1021/ie4000344.

(9) Zhu, X. X.; Asante, N. D. K. Diagnosis and Optimization Approach for Heat Exchanger Network Retrofit. AIChE J. 1999, 45, 1488−1503 DOI: 10.1002/aic.690450712.

(10) Suphanit, B. Design of Complex Distillation Systems. Ph.D. Thesis. University of Manchester Institute of Science and Technology, Manchester, UK, 1999.

(11) Gadalla, M. Retrofit Design of Heat-Integrated Crude Oil Distillation Systems. Ph.D. Thesis. University of Manchester Institute of Science and Technology, Manchester, UK, 2003.

(12) Rastogi, V. Heat-Integrated Crude Oil Distillation System Design. Ph.D. Thesis. The University of Manchester, Manchester, UK, 2006.

(13) MATLAB, R2012a; The MathWorks Inc., 2012.

(14) Liau, L. C. K.; Yang, T. C. K.; Tsai, M. T. Expert system of a crude oil distillation unit for process optimization using neural networks. Expert Syst. Appl. 2004, 26, 247−255 DOI: 10.1016/S0957-4174(03)00139-8.

(15) Maples, R. Petroleum Refinery Process Economics, 2nd ed.; Pennwell Corp.: Tulsa, OK, 2000.

(16) Douglas, J. M. Conceptual Design of Chemical Processes; McGraw-Hill International Ed.: New York, London, 1988.

(17) Peters, M. S., Timmerhaus, K. D. Plant Design and Economics for Chemical Engineers, 3rd ed.; McGraw-Hill International eds.: New York, London, 1980.

(18) SPRINT, V1.6; Department of Process Integration, University of Manchester Institute of Science and Technology: Manchester, UK, 2002.

(19) Petroleum and Other Liquids; EIA: Washington, DC, Aug 20, 2012; www.eia.gov/dnav/pet/pet_pri_spt_s1_d.htm (accessed Aug. 20, 2012).

(20) Liu, J. Predicting the Products of Crude Oil Distillation Columns. M.Phil. Thesis. The University of Manchester, Manchester, UK, 2012.

(21) Metropolis, N.; Rosenbluth, A. W.; Rosenbluth, M. N.; Teller, A. H.; Teller, E. Equation of State Calculations by Fast Computing Machines. J. Chem. Phys. 1953, 21, 1087−1092 DOI: 10.1063/ 1.1699114.

(22) Wolpert, D.; Macready, W. No Free Lunch Theorems for Optimization. IEEE Trans. Evol. Comput. 1997, 1, 67−82 DOI: 10.1109/4235.585893.

(23) Dolan, W. B.; Cummings, P. T.; Le Van, M. D. Process Optimization via Simulated Annealing: Application to Network Design. AIChE J. 1989, 35, 725−736 DOI: 10.1002/aic.690350504.

(24) Zhang, H.; Rangaiah, G. P. One-step approach for heat exchanger network retrofitting using integrated differential evolution. Comput. Chem. Eng. 2013, 50, 92−104 DOI: 10.1016/j.compche-meng.2012.10.018.

(25) Watkins, R. N. Petroleum Refinery Distillation, 2nd ed.; Gulf Publishing Company: Houston, TX, 1979.

(26) Yee, T. F.; Grossmann, I. E. Simultaneous optimization models for heat integration II. Heat exchanger network synthesis. Comput. Chem. Eng. 1990, 14, 1165−1184 DOI: 10.1016/0098-1354(90) 85010-8.

(27) Pan, M.; Bulatov, I.; Smith, R. New MILP-based iterative approach for retrofitting heat exchanger networks with conventional network structure modifications. Chem. Eng. Sci. 2013, 104, 498−524 DOI: 10.1016/j.ces.2013.09.049.

(28) Aspen HYSYS, V7.3; Aspen Technology Inc.: Bedford, MA, 2011.